J Nanostruct 6(3): 179-183, Summer 2016

RESEARCH PAPER

Enhanced luminescence of Er^{+3}-doped Zinc-Lead-Phosphate Glass embedded SnO_2 nanoparticles

Haydar Aboud

Baghdad College of Economic Sciences University, Iraq

ARTICLE INFO

Article History:
Received 8 May 2016
Accepted 17 June 2016
Published 1 July 2016

Keywords:
Amorphous materials
Energy band gap
Nanoparticles
Luminescence

ABSTRACT

Introduction of the nanoparticles in the bulk glass received a large interest due to their versatile application. The composition of Er^{+3}-doped Zinc-Lead-Phosphate glass samples are prepared by melt-quenching technique. The structural and optical properties of phosphate glass have been examined by x-ray diffraction, field emission scanning electron microscopy, photoluminescence spectroscopy and UV-Vis-NIR scanning spectrophotometer. The x-ray diffraction pattern has confirmed their amorphous nature and the field emission scanning electron microscopy micrograph showed the distribution of nanoparticles in glass. The study indicates that doped SnO_2 nanoparticles have an influence on the band gap energy that decreases with the increasing amount of nanoparticles. The photoluminescence spectra showed three peaks at the green-orange region of the visible spectrum and four times enhancement for doped 0.25% SnO_2 nanoparticles. The enhancement in the luminescence intensity of the green-orange region is found to be due to the effective local field of nanoparticles. The optical properties motivate to use these glassed as novel luminescent optical materials.

How to cite this article
Aboud H,. Enhanced luminescence of Er^{+3}-doped Zinc-Lead-Phosphate Glass embedded SnO_2 nanoparticles . J Nanostruct, 2016; 6(3):179-183. DOI: 10.7508/JNS.2016.03.001

INTRODUCTION

Recently, the rare-earth (RE) has been extensively studied due to its strong luminescence and high-brightness in the glass matrix, which has frequently used in optical communications [1-4]. However, the cross sections for optical excitation of RE ions are usually quite small and the radiative lifetimes of the excited states are long, resulting in low emission efficiency [5]. To overcome this problem and enhance the luminescence, nanoparticles can be used as co-doped with (RE) ions, which act as sensitizers (donor), so compensate the small cross-section of transitions of (RE) by energy transfer from nanoparticles to (RE) [6-10].

In recent, the synthesis and properties of heavy metal glasses co-doped nanoparticles (NPs) with rare earth have attracted several interests for optical applications [11-18]. The objective of the present work we have study influences of SnO_2 nanoparticles of Er^{+3} -doped Zinc-Lead-Phosphate glass on optical properties systems.

* *Corresponding Author Email: han55608@yahoo.com*

MATERIALS AND METHODS

The glass samples were prepared with a nominal composition of (59-x) P_2O_5-20ZnO -20Pb-1Er_2O_3-xSnO_2 with x = (0, 0.1, 0.25 and 0.5) by using melt quenching technique. The SnO_2 nanoparticles of size about 22-31 nm were synthesized by sol-gel method [19]. Table 1 shows the various composition of the sample. The batches of 15 g of the mixed raw materials of phosphoric acid (H_3PO_4, 99%), zinc oxide (ZnO, 99.7%), lead oxide

Table 1. Nominal composition in percentage (%) of (59-x) P_2O_5-20ZnO -20Pb-1Er_2O_3-xSnO_2 glass system

	P_2O_5 (%)	ZnO (%)	PbO (%)	Er_2O_3 (%)	SnO_2(%)
G1	59	20	20	1	0
G2	58.9	20	20	1	0.1
G3	58.75	20	20	1	0.25
G4	58.5	20	20	1	0.5

(PbO, 99%), erbium oxide (Er_2O_3, 99.8%) were put in a platinum crucible and melted at 990C for one hour in a furnace under atmospheric pressure. The samples were placed between two brass plates for quenching and then cooled down at room temperature. The phase purity and phase structure of powder samples were characterized by the X-ray powder diffraction (patterns) with Cu-K_α radiation operating at 40 kV, 30mA at room temperature using Siemens Diffractometer D5000, equipped with diffraction software analysis. The morphology was examined by using field emission scanning electron microscopy. The measurement of the optical absorption and the absorption edge were done by using the UV-Vis-NIR scanning spectrophotometer. The Perkin Elmer LS55 Luminescence spectrometer was used to determine the photoluminescence properties of the doped glass.

RESULTS AND DISCUSSION

Fig. 1 shows the result of x-ray Diffraction (X-ray) of the glass sample. This pattern (the presence of diffuse peak and absence of the sharp peak) indicates that the glass is totally amorphous. The FE-SEM images of a glass are used to investigate the microstructures of the Er^{+3} doped of ZnO–Pb-P_2O_5 with co-doped SnO_2 nanoparticles. The cross-sectional FE-SEM image of the glass is presented in Fig. 2(A) which shows the absence of SnO_2 nanoparticles in the glass. The high magnification image (Fig. 2(B)) reveals the same sample and confirms the presence of SnO_2. Fig. 2(c) depicts the average and uniform size distribution of SnO_2 nanoparticles (~21nm).

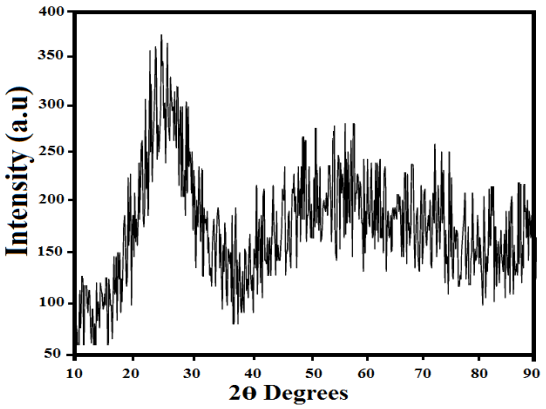

Fig. 1. XRD pattern obtained for Er^{+3} doped of ZnO–Pb-P_2O_5 glass with SnO_2 nanoparticles.

Absorption spectrum of Er^{+3}doped of ZnO–Pb-P_2O_5 glasses with and without SnO_2 nanoparticles is illustrated in Fig. 3. The six absorption peaks in the range of 485 to 1536 nm can be seen clearly. The peaks at 1536, 979, 799, 650, 523, and 485 nm correspond to absorption from $^4I_{15/2}$ ground state to $^4I_{13/2}$, $^4I_{11/2}$, $^4I_{9/2}$, $^4F_{9/2}$, $^2H_{11/2}$ and $^4F_{7/2}$ energy levels of Er^{3+} ions respectively. No peaks shift was observed after embedding SnO_2 nanoparticles in the host matrix. The indirect energy band gaps are plotted between $(aE)^{1/2}$ and (E) for each sample (Fig. 4(A)). The direct, indirect energy band gaps and Urbach energy values for glass composition are listed in Table 2. Fig.4(B) shows the indirect band gaps decreases with increasing content of SnO_2 nanoparticles. This behavior in band gaps is attributed to the change in structure, i.e. increase in non bringing oxygen with the addition of SnO_2 nanoparticles. Furthermore, the SnO_2 nanoparticles can produce a new energy levels located in the gap of glass.

The photoluminescence spectra of Er^{+3} doped of ZnO–Pb-P_2O_5 with co-doped SnO_2 nanoparticles glasses was measured at excitation 797 nm. Fig. 5A shows the influence of various concentration of SnO_2 on emission spectra of Er^{+3}. The enhancement in intensities of the up conversion emissions were increased (`4 times) with increasing SnO_2 concentrations from 0.1to 0.25.

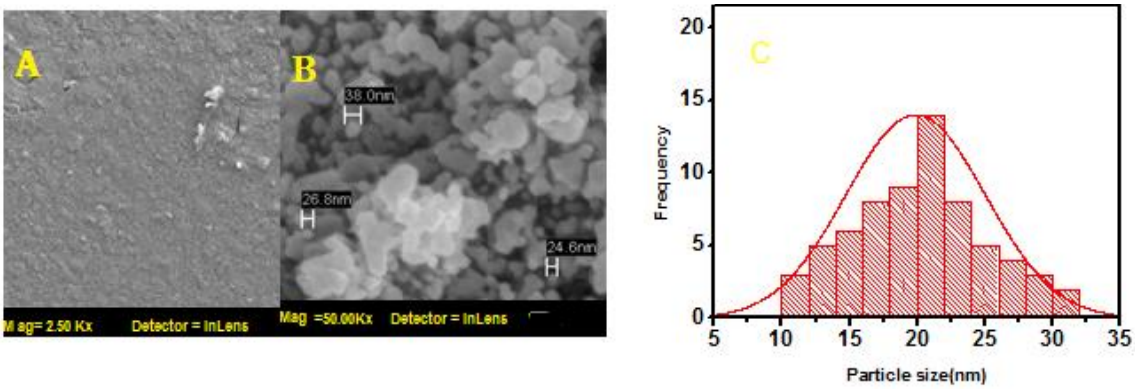

Fig. 2 (A). Cross-sectional FE-SEM image of the 1 mol% Er^{+3} and 0.25 mol% SnO_2 co-doped, (B) high resolution FE-SEM image of the same sample, and (C) size distribution of SnO_2 nanoparticles.

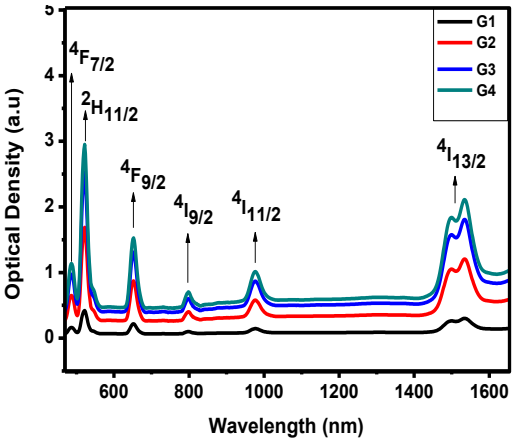

Fig. 3. Absorption spectra of Er^{+3} doped of ZnO–Pb-P_2O_5 glass with co-doped SnO_2 nanoparticles.

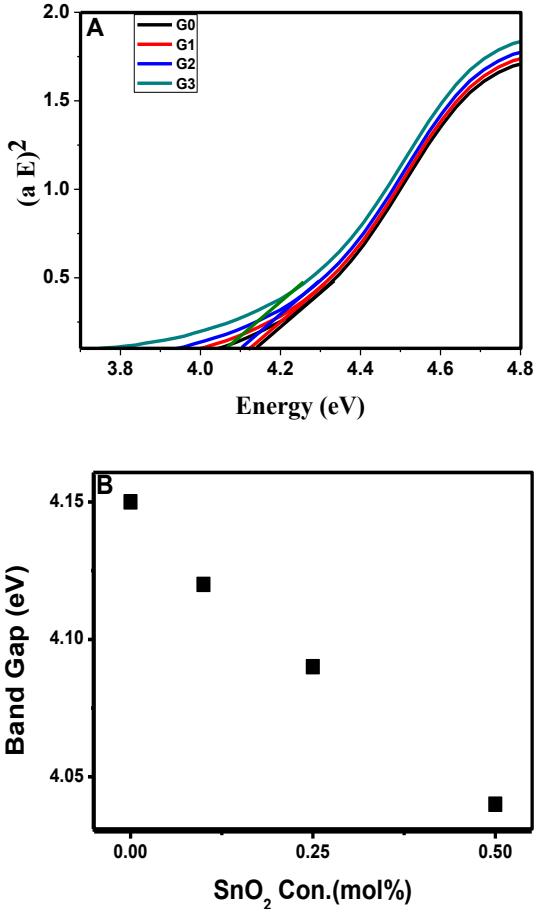

Fig. 4.(A) indirect optical band gap plot of glass with different concentration of SnO_2 nanoparticles, (B) Variation of band gap with different concentration of SnO_2 nanoparticles.

This behavior is may be due to following defects in the host material. The most common defect of the oxygen vacancies act as radiative centres in the host and the energy transfer process between SnO_2 nanoparticles and Er^{+3} ions. Moreover, the quenching phenomena were observed with an increasing content up to 0.5. This phenomenon is due to the increasing agglomeration of nanoparticles, decreasing the surface-to-volume ratio, and the energy transfer from Er^{+3} to the surface of SnO_2 nanoparticles. Furthermore, the three emission bands in the wavelength ranging from 470 to 650 nm observed at 502, 545 and 606 respectively. Fig. .5B reveals the enhancement factor of the different transitions.

The energy level diagram (Fig.6) for Er^{+3}shows the up-conversion emission, excited state absorption (ESA) and energy transfer (ET). The excitation energy converts to up-conversion luminescence spectra by sequential absorption of photons from ground state ($^4I_{15/2} \rightarrow {}^4I_{9/2}$). The non-radiative losses and multi-phonon relaxations can be observed at ($^4I_{9/2} \rightarrow {}^4I_{11/2}$, $^4I_{11/2} \rightarrow {}^4I_{13/2}$, $^4I_{7/2} \rightarrow {}^2H_{11/2}$ and $^2H_{11/2} \rightarrow {}^4S_{3/2}$). The probability of energy

Table 2. Direct (E_{dir}), indirect (E_{indir}) energy band gaps and Urbach energy (E_{tail}) of ZnO –Pb- P_2O_5 glass doped with Er_2O_3 and SnO_2 nanoparticles

No. sample	G1	G2	G3	G4
E_{dir} (eV)	4.28	4.17	4.14	4.1
E_{indir} (eV)	4.15	4.12	4.09	4.04
E_{tail} (eV)	0.16	4.12	4.09	4.04

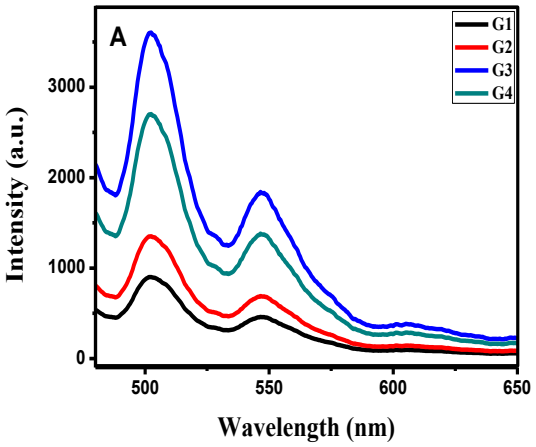

Fig. 5.(A) Up-conversion emissions of Er^{+3} doped ZnO–Pb-P_2O_5 glass with co-doped SnO2 nanoparticles. (B) Normalized intensity of fluorescence related to different SnO_2 concentration.

transfer (ET) between two neighboring Er^{+3} ions is indicated at ($^4I_{11/2} \rightarrow {}^4I_{15/2}$) non-radiative decay, and ($^4I_{13/2} \rightarrow {}^9F_{9/2}$), ($^4I_{11/2} \rightarrow {}^4I_{7/2}$) transfer the energy to another one. Moreover, the three prominent emission spectra are observed according to the following transitions (green: $^2H_{11/2} \rightarrow {}^4I_{15/2}$), (green: $^4S_{3/2} \rightarrow {}^4I_{15/2}$) and (orange: $^4I_{9/2} \rightarrow {}^4I_{15/2}$).

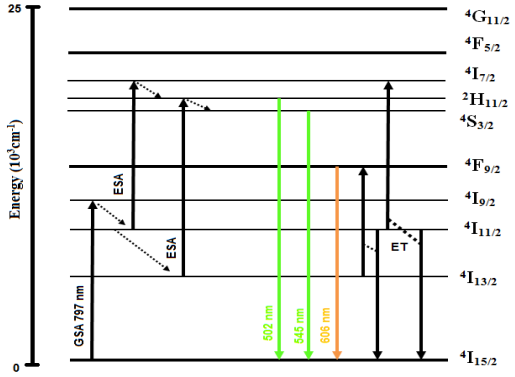

Fig. 6. Absorption and Emission energy levels diagram Er^{+3} doped P_2O_5 - ZnO -Pb glass with co-doped SnO_2 nanoparticles.

CONCLUSION

The Er^{+3}-doped Zinc-Lead-Phosphate Glass with co-doped SnO_2 nanoparticles were synthesized using melt quenching technique. Their optical absorption and luminescent properties were studied here. The direct and indirect band gap decreases with increasing the SnO_2 concentration. The emission spectrum (green at 502nm, green at 545nm and orange at 606nm) has been observed with excitation at 797nm of Er^{+3}. The enhanced intensity with increasing SnO_2 nanoparticles has also been observed. These glasses could be used for the development of solid-state lasers.

REFERENCES

1. Weber MJ. Science and technology of laser glass. J Non-Cryst Solids. 1990;123(1–3):208-22.
2. Chen W, Bovin J-O, Joly AG, Wang S, Su F, Li G. Full-Color Emission from In2S3 and In2S3:Eu^{3+} Nanoparticles. Phys. Chem. B. 2004;108(32):11927-34.
3. Najar A, Charrier J, Lorrain N, Haji L, Oueslati M. Optical gain measurements in porous silicon planar waveguides codoped by erbium and ytterbium ions at 1.53µm. Appl. Phys. Lett. 2007;91(12):121120.
4. Vela J, Prall BS, Rastogi P, Werder DJ, Casson JL, Williams DJ, et al. Sensitization and Protection of Lanthanide Ion

Emission in In_2O_3:Eu Nanocrystal Quantum Dots. J. Phys. Chem. C. 2008;112(51):20246-50.
5. Zhang X, Lin T, Jiang X, Xu J, Liu J, Xu L, et al. Photoluminescence from Er^{3+} ion and SnO_2 nanocrystal co-doped silica thin films. COL. 2012;10(9):091603-.
6. Jose G, Jose G, Thomas V, Joseph C, Ittyachen MA, Unnikrishnan NV. Fluorescence enhancement from Eu^{3+} ions in CdSe nanocrystal containing silica matrix hosts. Mater. Lett. 2003;57(5–6):1051-5.
7. Ishizumi A, Kanemitsu Y. Structural and luminescence properties of Eu-doped ZnO nanorods fabricated by a microemulsion method. Appl. Phys. Lett. 2005; 86(25): 253106.
8. Lin C-C, Lin K-M, Li Y-Y. Sol–gel synthesis and photoluminescent characteristics of -doped nanophosphors. Journal of Luminescence. 2007;126(2):795-9.
9. Wan N, Xu J, Lin T, Zhang X, Xu L. Energy transfer and enhanced luminescence in metal oxide nanoparticle and rare earth codoped silica. Appl. Phys. Lett. 2008;92(20):201109.
10. Weber MJ, Myers JD, Blackburn DH. Optical properties of Nd^{3+} in tellurite and phosphotellurite glasses. J. Appl. Phys. 1981;52(4):2944-9.
11. Dousti MR, Sahar MR, Ghoshal SK, Amjad RJ, Arifin R. Up-conversion enhancement in Er^{3+}-Ag co-doped zinc tellurite glass: Effect of heat treatment. Journal of Non-Crystalline Solids. 2012;358(22):2939-42.
12. Zhang WF, Yin Z, Zhang MS, Du ZL, Chen WC. Roles of defects and grain sizes in photoluminescence of nanocrystalline SrTiO 3. J. Phys. Condens. Matter. 1999;11(29):5655.
13. Brovelli S, Galli A, Lorenzi R, Meinardi F, Spinolo G, Tavazzi S, et al. Efficient 1.53 μm erbium light emission in heavily Er-doped titania-modified aluminium tellurite glasses. Journal of Non-Crystalline Solids. 2007;353(22–23):2150-6.
14. Marjanovic S, Toulouse J, Jain H, Sandmann C, Dierolf V, Kortan AR, et al. Characterization of new erbium-doped tellurite glasses and fibers. Journal of Non-Crystalline Solids. 2003;322(1–3):311-8.
15. Gu F, Wang SF, Lü MK, Qi YX, Zhou GJ, Xu D, et al. Luminescent characteristics of Eu^{3+} in SnO_2 nanoparticles. Opt. Mater. 2004;25(1):59-64.
16. Elhouichet H, Othman L, Moadhen A, Oueslati M, Roger JA. Enhanced photoluminescence of Tb^{3+} and Eu^{3+} induced by energy transfer from SnO2 and Si nanocrystallites. Mater. Sci. Eng. B. 2003;105(1–3):8-11.
17. Castillo JD, Rodríguez VD, Yanes AC, Méndez-Ramos J, Torres ME. Luminescent properties of transparent nanostructured Eu 3+ doped SnO_2 –SiO_2 glass-ceramics prepared by the sol–gel method. Nanotechnology. 2005;16(5):S300.
18. Aboud H, Wagiran H, Hossain I, Hussin R, Saber S, Aziz M. Effect of co-doped SnO_2 nanoparticles on the optical properties of Cu-doped lithium potassium borate glass. , Mater. Lett. 2012;85:21-4.
19. Aziz M, Saber Abbas S, Wan Baharom WR. Size-controlled synthesis of SnO_2 nanoparticles by sol–gel method. Mater. Lett. 2013;91:31-4.